Porous Gold Surfaces for Implantable Neural Electrodes

Helen Edström

November, 2014

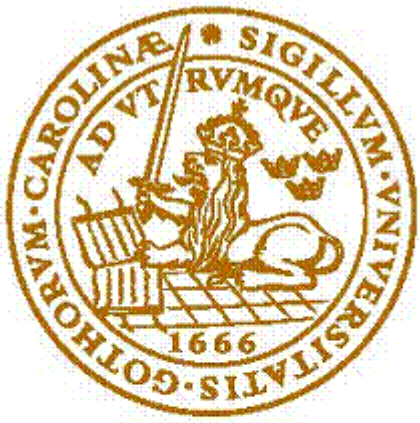

LUND
UNIVERSITY

Master´s Thesis

Faculty of engineering, LTH
Department of Biomedical Engineering

Supervisor: Fredrik Ejserholm
Co-supervisor: Martin Bengtsson
Examiner: Lars Wallman
Opponents: Marcus Jönsson and Jennifer Linge

Contents

1 Abstract

Neural electrodes used for measurements of action potentials in brain cells are often made of gold. These electrodes need to be sufficiently small to cover only one brain cell, but this induces the problem of increased impedance since impedance scales inversely with surface area. This means that if the surface area is too small, only noise will be measured. One way to overcome this problem is to try to enlarge the real surface area by making the gold nanoporous. In this way, the geometric surface area can be kept small while the real surface area becomes several times larger.

In this project, attempts to increase the surface area by anodization has been made. First, a silicon wafer with a large number of chips containing six electrodes each was fabricated using techniques such as evaporation, *UV* exposure and etching. Then the chips were diced out of the wafer and each chip was glued onto a circuit board. The copper and gold were connected by a thin aluminum wire and covered by silicone for protection and isolation.

Different anodization modes and times were tested on the electrodes, and the results were evaluated by both an optical microscope and a *SEM*. At the best combination of anodization mode and time, the impedance was measured both before and after anodization. Also, cyclic voltammetry was used in order to calculate the real surface area of the electrodes.

The results of the measurements show an increase of the real surface area with up to approximately seven times. This was confirmed by the impedance measurements, which clearly showed that the impedance sharply decreased after anodization compared to the impedance measured before anodization. This indicates that surface enlargement of gold electrodes by anodization is a viable method, but it should be carried out on more electrodes in order to get reliable results.

2 Sammanfattning på svenska

Neurala elektroder som används för mätning av aktionspotentialer i hjärnceller är ofta gjorda av guld. Dessa elektroder måste vara tillräckligt små för att täcka endast en hjärncell, men detta medför problemet med ökad impedans eftersom impedans är omvänt proportionell mot ytarea. Detta innebär att om ytarean är för liten mäts endast brus. Ett sätt att överkomma detta problem är att försöka förstora den verkliga ytarean genom att göra guldet nanoporöst. På detta sätt kan den geometriska ytarean hållas liten medan den verkliga ytarean blir flera gånger större.

I det här projektet har försök gjorts att öka ytarean genom anodisering. Först tillverkades en kiselskiva med ett stort antal chip som vardera innehöll sex elektroder med hjälp av tekniker så som evaporering, *UV*-exponering och etsning. Sedan sågades chippen ut ur skivan och varje chip limmades fast på ett kretskort. Kopparn och guldet sammankopplades via en tunn aluminiumtråd och täcktes med skyddande och isolerande silikonlim.

Olika anodiseringssätt och -tider testades på elektroderna och resultaten utvärderades med hjälp av både optiskt mikroskop och *SEM*. Vid den bästa kombinationen av anodiseringssätt och -tid mättes impedansen både före och efter anodisering. Även cyklisk voltammetri användes för att beräkna elektrodernas verkliga ytarea.

Resultaten av mätningarna visade en ökning av den verkliga ytarean med upp till ungefär sju gånger. Detta bekräftades av impedansmätningarna, som tydligt visade att impedansen kraftigt minskade efter anodisering jämfört med impedansen som mättes innan anodisering. Detta indikerar att ytförstoring av guldelektroder via anodisering är en gångbar metod, men det bör göras på fler elektroder för att få ett tillförlitligt resultat.

3 Acknowledgements

I was able to do this Master´s Thesis thanks to some certain people, and I would like to express my gratitude to them.

First of all, I would like to thank my supervisors, Fredrik Ejserholm and Martin Bengtsson, for giving me the opportunity to do this Master´s Thesis. Thank you for your support and encouragement, it has been a very interesting project. Thank you also for helping me with fabrication, using different machines and text improvements.

I also want to thank the personnel and the other M.Sc. stundents at the division of Biomedical Engineering. I truly enjoyed our fika times in the lunch room.

Finally, I would like to thank my family and friends for always being there for me. And last, but not least, I want to thank Kim, the love of my life, for always supporting me, believing in me and cheering me up when I am feeling down. And also, thanks for all your help with MATLAB and LaTeX. Everyone who has proofread my report, thanks to you too.

Helen Edström

Lund, November 2014

4 Introduction

4.1 Neural signaling

The cells in the human body are in need of electrical activity to function properly. Electrical signals are generated by the neurons (nerve cells) and they transmit information through the axons in the nervous system. The neurons utilize the ions (e.g. of sodium and potassium) diffusing across their plasma membrane due to concentration gradients.

The axons are rather long (they can exceed $1m$) and, furthermore, they are quite bad electrical conductors. This entails a problem for the neurons when it comes to transmitting electrical signals, but to overcome this problem, they have an auxiliary system that produces electrical signals called action potentials, which are transitory changes (they last for approximately $1ms$) from negative to positive in the transmembrane potential, see Figure 1. The action potentials are propagating along the axons and can travel far even though the axons lack conductivity properties.

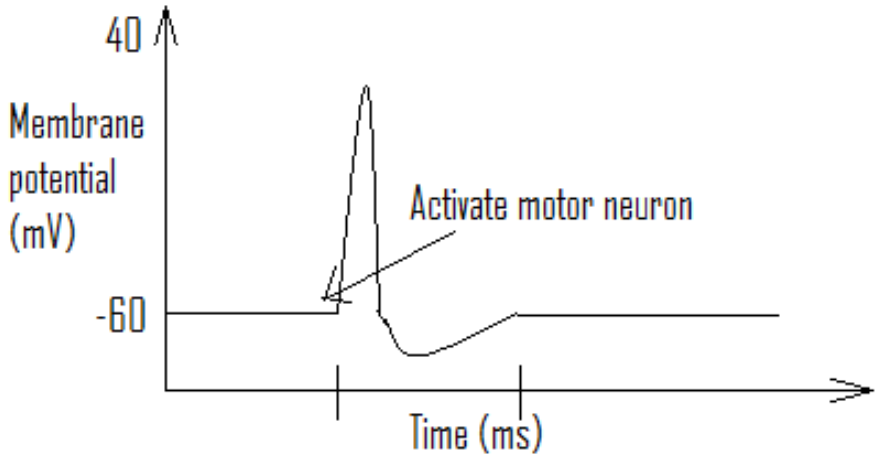

Figure 1: *Schematic drawing of a recorded action potential.*

Neurons generally generate a so called resting membrane potential. By recording the potential between the interior and the exterior of the neurons, this potential can be measured. The resting membrane potential is negative, but the action potential momentarily obliterates it, making the potential across the membrane positive.

To observe the action potentials, one can measure the electrical potential across

the plasma membrane of the neurons using an intracellular microelectrode. This type of electrode usually consists of a thin, tapered glass tube with an opening diameter smaller than $1\mu m$, packed with a concentrated salt solution or some other material that conducts electricity well. When the microelectrode enters the cell, it detects a negative potential, due to a constant voltage generated across the cell membranes when the cells are at rest, i.e. the resting membrane potential. This potential ranges from -40 to $-90mV$.

Action potentials can be stimulated by passing electrical current across the neuron membrane. It is also possible to produce action potentials in a laboratory by using two microelectrodes inserted into the same neuron and connecting the second electrode to a battery. The current delivered in this manner can be either more negative (causing hyperpolarization) or positive (causing depolarization) than the membrane potential. In the former case, the membrane potential adjusts to the magnitude of the injected current, but nothing drastically happens. In the latter case, on the other hand, the membrane potential of the neuron becomes more positive than the resting potential and at a certain threshold potential, an action potential arises. The hyperpolarizing responses are called passive electrical responses and the depolarizing responses (giving rise to the action potential) are called active electrical responses.

The magnitude of the current does not determine the amplitude of the action potential. If the current is high or the duration of the stimulation is long, the action potentials will not be larger, but several successive action potentials might occur. The reason why electrical potentials occur in the neurons is that the difference in ion concentration between the interior and the exterior of the cell forces ions to diffuse through the membrane. The cell membrane is selectively permeable to some ions, and if the concentration of a specific type of ion is higher on e.g. the inside of the cell compared to the outside of the same cell, the electrical potential of the inside will be negative relative to the electrical potential of the outside [1].

The number of neurons in the brain of an adult human is approximately $8.5{\cdot}10^{10}$, connected by approximately 10^{14} synapses and using about 100 chemical neurotransmitters. The number of neurons in a neural circuit can be in the order of $10^3 - 10^5$. Since the brain works at the nanoscale, the tools for studying it should also operate at the nanoscale. Many brain diseases, like schizophrenia, depression, epilepsy and Parkinson´s disease, can be treated using implanted neural electrodes [2].

4.1.1 Neuronano Research Center

At the Faculty of Medicine at Lund University, there is an interdisciplinary research and innovation center called Neuronano Research Center (*NRC*). At this center, neuroscience (both *in vivo* and *in vitro*) is combined with organic chemistry and technology at the micro- and nanoscale in order to develop a new generation of neural interfaces that can communicate with the nervous system. *NRC* conducts basic research as well as developing clinical applications and the researchers working there come from different faculties, such as medicine, engineering, science and humanities [3].

A neural electrode used for implantation at the *NRC* consists of gold covered polyimide and it has the shape of an isosceles triangle with one side of $5-10\mu m$ and two sides of $5-7\mu m$. The area of a triangle with the sidelengths a, b and c, is given by Equation 1 (Heron´s formula). The s in this equation is given by Equation 2 [4].

$$A = \sqrt{s(s-a)(s-b)(s-c)} \tag{1}$$

$$s = \frac{1}{2}(a+b+c) \tag{2}$$

For an isosceles triangle (where $a = c$ in Heron´s formula), the equation is simplified to Equation 3.

$$A = \frac{b}{4}\frac{\sqrt{4a^2-b^2}}{2} \tag{3}$$

This gives the neural electrode a surface area in the range of approximately $5.4-12.2\mu m^2$ (side lengths of $5\mu m$, $5\mu m$, $5\mu m$ and $7\mu m$, $7\mu m$, $10\mu m$, respectively). Mostly, the surface area of these electrodes is about $12-13\mu m^2$.

4.2 Background and aims of this Master´s Thesis

This Master´s Thesis is a continuation of the Master´s Thesis *Fabrication of a porous anodic alumina membrane* (2013) by Josefin Nissa [5]. In her Master´s Thesis, she made attempts to fabricate a porous anodic alumina membrane on gold electrodes after evaporating an aluminum layer onto them, using anodization, and deposit an electrically conductive polymer onto the electrode surface, using the aforementioned membrane as a scaffold to produce polymer wires. The membrane would then be dissolved and the polymer wires on the electrode

would provide an enlarged surface area.

The original aluminum had a rough surface though, and it seemed to loosen from the electrode after long-time exposure to the acid. On the other hand, the surface beneath the aluminum, i.e. the gold, had been affected by the anodization and exhibited a structural change at the surface. The gold had become porous!

In this Master´s Thesis, the aim was to fabricate nanoporous electrodes, using the gold electrodes directly and creating a nanoporous surface on them by anodization. In the first step, different combinations of anodization modes and times were supposed to be tested to find out which mode of anodization and for how long time that gives the best resulting surface structure. This combination would then be used in the second step, where the impedance of the electrodes would be measured before and after anodization in order to investigate whether the impedance decreases after anodization (which is desirable, since that would indicate an enlarged surface area). Also, the surface area of the electrodes would be calculated after anodization to investigate whether the surface area has increased (by comparing it to the geometric surface area).

4.3 The method of choice

4.3.1 Chip fabrication

To manufacture the electrodes, the chosen method was to use a silicon wafer with a thin layer of titanium and a thick layer of gold deposited onto it and to etch the structures using a photomask. The wafer would then be covered by a quite large number of chips containing six electrodes each. The chips would be diced out of the wafer using a special dicing machine and each chip would be glued onto a circuit board. To connect the electrode to the circuit board to enable current to pass through the electrode, a thin aluminum wire would be attached to the gold electrode and the corresponding copper conductor, like a bridge, with help from a wirebond machine. To protect and isolate the wires, a silicone would cover part of the sample.

4.3.2 Measurements

The electrodes would then be anodized to form nanoporous gold surfaces. Different anodization modes (potentiostatic and galvanostatic) and times would be tested in order to compare the electrodes and investigate which combination that gives the best results. They would be investigated both with an optical microscope and with a scanning electron microscope (*SEM*). The anodization

mode-time combination providing the best resulting surface structure would be repeated, and impedance measurements would be performed before and after this anodization step. After anodization, the real surface area would be measured and compared to the geometric surface area.

4.4 Currently used surface enlargement method

A surface area enlargement method for electrodes used currently is platinum electroplating, meaning the electrode surface is covered by a thin layer of platinum via electrolysis. This method gives a rough surface, similar to cauliflower, and this structure is called platinum black. The surface area becomes large enough, but a disadvantage is that the platinum adheres poorly to the electrode and might loosen, which is of course a problem when it comes to electrodes implanted in the brain [6].

5 Theory

5.1 Nanoporous gold

Nanoporous gold has many properties that make it attractive for several applications (e.g. catalysis, fuel cells and biosensors [7]), such as large surface area, high conductivity, biocompatibility and stability [8]. It is also very durable, with the ability to sustain macroscopic stresses as high as $200MPa$ [9]. The real surface area of nanoporous gold is several times larger than the real surface area of planar gold with the same geometric surface area, usually about $15-25$ times larger. Due to the larger surface area, nanoporous gold is more conductive than planar gold, because there are more sites for electron transfer to occur, due to a larger surface area, and this action is hindered on planar gold [10].

One application is nanoporous gold electrodes, containing a bicontinuous three-dimensional network of pores and ligaments on the nanoscale. These electrodes are highly conductive and have, due to their roughness, a much larger surface area than planar gold electrodes of the same geometric size, see Figure 2. The surface area may vary from twice as large to a thousand times as large, depending on the degree of porosity. The smaller the pore size, the larger the surface area. Smaller pores also indicate higher catalytic activity [11]. Electrochemical deposition or dealloying is another way to create nanoporous gold. The latter method provides a high mechanic integrity for the film [12]. It is also possible to roughen or etch planar gold electrodes to increase their porosity [11]. Nanoporous gold can also be obtained from binary gold alloys, where the more chemically active element in the alloy is selectively removed. Simple microfabrication techniques can be used to prepare nanoporous gold usable in the field of electrochemistry [13]. Electrochemical deposition can also be utilized and electrochemical dealloying provides nanoporous gold films with high mechanical integrity [12].

Figure 2: *Schematic drawing of planar gold, above, compared to nanoporous gold, below, of the same geometric size. It can easily be seen that the real surface area is significantly larger for the porous gold than for the planar gold.*

In order to "listen" to a particular brain cell with a neural electrode, the electrode must be small enough to only cover the cell in question. It should not cover several cells since that would make it difficult to distinguish which one of the cells that is the active one. There is also a risk of short-circuiting two cells if the electrode is too large. A disadvantage with decreasing the size of the electrode is that the impedance, which scales inversely with the surface area of the electrode, becomes too high, decreasing the signal-to-noise ratio (S/N). For instance, at $1kHz$, the impedance is $850k\Omega$ for conventional gold electrodes but only $30k\Omega$ for nanoporous gold electrodes [14], in other words, only a few percent of the impedance for the conventional electrodes (of the same geometric size). The impedance should be as low as possible in order to keep the noise at a low level when the electrode is used as a sensor. This is where nanoporous gold electrodes are useful; they have a much higher surface area-to-volume ratio than planar gold, reducing the impedance more than tenfold. In other words, when it comes to electrochemistry, nanoporous gold electrodes have a great potential. The preferable diameter of the pores is in the range of $30 - 40nm$ [13].

The pore size on a porous electrode is not uniform; there is a range of pore dimensions. Part of the surface area is outside of the pores and since gold is a noble metal, the electrodes are stable. Furthermore, gold has a wide range of ideal polarizability and the mobility of gold atoms is high, giving bulk gold a high melting temperature ($1053°C$) [15]. Nanoporous gold, on the other hand, has a much lower melting point than bulk gold due to its higher surface area-to-volume ratio providing different thermal and thermodynamic properties [16].

The current generated by oxidation or reduction of a chemical substance at the electrode is called the Faradaic current [17]. The non-Faradaic current represents the noise in electrochemistry, and like Faradaic current, it increases with decreasing electrode area (other parameters remain constant) [11]. The degree of electrode porosity affects the Faradaic peak current [18].

The impedance Z is given by Ohm´s law [19], see Equation 4,

$$V = ZI \tag{4}$$

where V is the potential and I is the current. As can be seen in this equation, if the potential is held constant, the current must be increased in order to decrease the impedance. If instead the current is held constant, decreasing the potential will also decrease the impedance.

5.2 Fabrication of nanoporous gold

Since oxalic acid can reduce gold oxide to gold atoms, it is possible to create nanoporous gold films using strong anodization of pure gold substrates in an aqueous solution of this acid. The gold surface is oxidized instantly when a high anodic potential is turned on, forming a thick gold oxide layer. The oxalic acid reduces this layer to gold atoms chemically, and these gold atoms easily form gold nanoparticle aggregates. The colour of the gold is different depending on whether the gold is in bulk form or nanoporous. A thick layer of gold oxide appears red, while black indicates a nanoporous gold film, meaning that this colour change confirms the reduction of generated gold oxide multilayer, which is important in the fabrication of nanoporous gold films [20]. To create nanoporous gold films, acidification is not necessary [21]. No surface modification is needed either [10].

There are mainly two modes of anodization: potentiostatic, where a constant potential is applied and the current is measured as a function of time, and galvanostatic, where a constant current is applied and the potential is measured as a function of time [22]. Studying the resulting graphs, it is possible to determine how the impedance changes with time, according to Equation 4, when either the potential or the current is held constant.

5.3 Applications and recent research

Porous gold is a versatile material with many applications, for instance optical biosensors [23], cell imaging [24], fuel cells [7] and electrodes [11]. During the last years, various articles regarding nanoporous gold and neural electrodes have been published. For instance, last year, Alivisatos et al [2] published an article dealing with the *Brain Activity Mapping Project* (*BAM*), which is about creating nanotools for neuroscience applications, focusing on both chemical neurotransmission and dynamic potential activity. The goal of this project is threefold:

1. The tools should be able to measure the activity of a large number of neurons in intricate brain circuits.
2. The brain circuits should be analyzed and modelled computationally.
3. The models should be tested by manipulation of activity of selected groups of neurons in the brain circuits.

Furthermore, the authors write that it is possible to produce implantable devices which are less intrusive due to the great size reduction of electronic systems

taking place during the last years. Thanks to this, tiny electrophysiological measurement tools for individual neurons can be developed. In the article, it is also mentioned that the impedance of the electrodes is the main physical barrier that determines the minimum sizes of intracellular neural interfaces. When it comes to extracellular measurements, it is even more essential, since the S/N is determined by the impedance of the electrodes and affects their sensitivity.

Another thing the authors mention is that extracellular microelectrodes are well-suited for BAM since they do not have to penetrate the neurons to record electrical signals. They are inserted in the brain and the distance between the cell bodies and the microelectrode surface within which electrical activity can be detected is typically about $50\mu m$.

5.3.1 Patent on porous gold materials and production methods

In September 2010, Nishio and Masuda published a patent on porous gold materials and production methods for them [25]. In their patent, they state that an aqueous solution of a carboxylate or a carboxylic acid (monovalent, divalent or trivalent) should be used for the anodization. A number of carboxylic acids that can be used are listed, namely acetic acid, citric acid, formic acid, lactic acid, maleic acid, malic acid, malonic acid, oxalic acid, propionic acid, succinic acid and tartaric acid, while the carboxylate salt can be chosen from any of the corresponding acids. The concentration of the acid used varies, e.g. $3.0M$ for citric acid and $0.6M$ for oxalic acid, both at room temperature. The higher the concentration, the higher the rate of formation of the porous film.

Any potential or current applied between the electrodes will do (as long as the potential is not so high that the gold on the electrodes is extricated), but the interval for the applied potential would be $1.5-11V$ (preferably $2-7V$), forming a uniform porous gold film with a pore size in the magnitude of $1-100nm$. With an aqueous solution of oxalic acid, the potential interval would be constrained to $2-5V$, while it would be $3-6V$ for citric acid.

The anodizaion time is not limited. Longer time provides a thicker porous film, up to a certain limit. At this limit, e.g. in case of using oxalic acid, the thickness does not increase anymore and further electrolysis in this situation may cause extrication of the film. Citric acid can provide thicker porous films than oxalic acid. Temperature affects the thickness of the porous film indirectly since higher temperature entails a faster process.

Due to the low potential applied and the fact that most of the carboxylic acids mentioned are harmless to humans, the production methods described in this

patent are safe.

5.4 Impedance measurements

There are two ways to measure the electrical impedance. It can be measured either potentiostatically (the potential is held constant and the current is varied) or galvanostatically (the current is held constant and the potential is varied) [26]. In both of these modes, both the potential and the current applied are measured and from Ohm´s law (Equation 4), the complex impedance, Z, can be calculated. Generally, the impedance is measured at different frequencies, see Figure 3. As can be seen in this figure, the impedance decreases with increasing frequency while the phase stays approximately constant (in the figure, there might be some disturbance at high frequency that makes the phase behave differently).

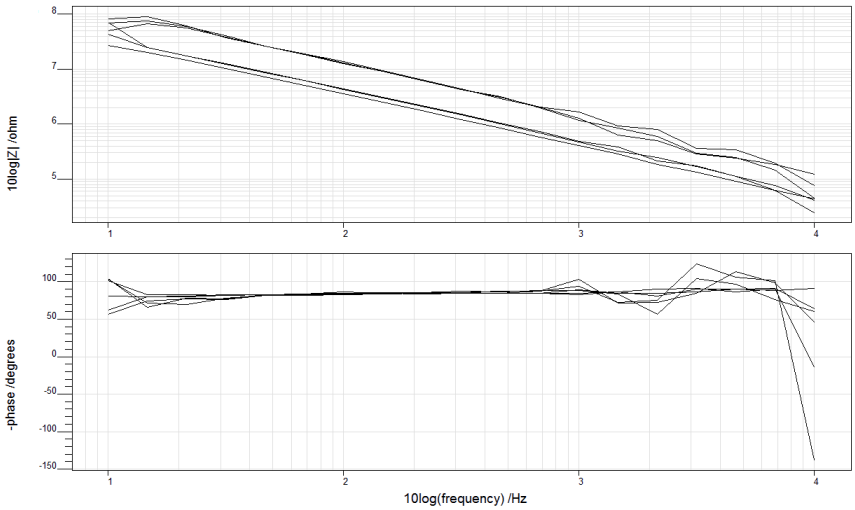

Figure 3: *Example of a potentiostatic impedance measurement as a function of frequency (above) and the phase as a function of frequency (below), measured before anodization (one curve for each electrode on the chip).*

5.5 Cyclic voltammetry

Cyclic voltammetry (CV) is a multipurpose technique used in electroanalysis for studying electroactive species. In this technique, the potential is first swept from a start potential to an end potential and then swept back to the start potential again. CV is mainly used in electrochemistry, but also in biochemistry, organic chemistry and inorganic chemistry. The method is to cycle the potential of an

electrode submerged in solution while measuring the current. The electrode to be investigated is called the working electrode. A reference electrode is also used for comparison. Figure 4 shows a schematic drawing of a typical CV graph. The signal sweeps between two potentials called the switching potentials. First, it scans negatively vs the reference electrode and after a certain time, it scans positively vs the reference electrode (reversed scan direction) [27].

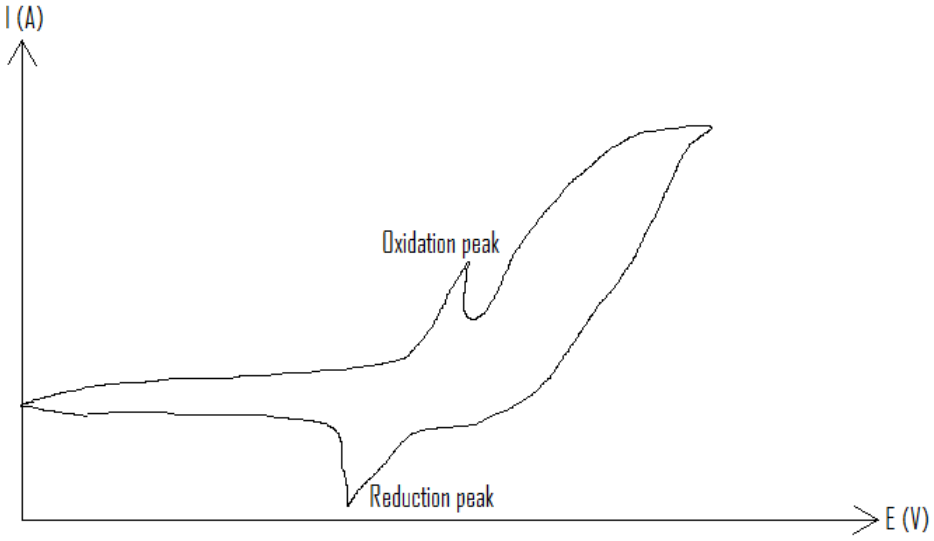

Figure 4: *Schematic drawing of a typical cyclic potential sweep curve. The current, I, is measured as a function of the potential, E. At the oxidation peak, oxygen is formed, and at the reduction peak, hydrogen is formed.*

When an electrode in an aqueous solution is exposed to sufficiently negative potentials, hydrogen adsorption on the electrode will occur. At positive potentials, there is an "oxygen region" and at negative potentials, there is a "hydrogen region" [28].

5.5.1 Calculation of the real surface area

One thing CV can be used for is to calculate the real surface area of an electrode. To calculate the real surface area, the potential is swept from a start value to different end values and the area under the curve (AUC) of the reduction peak is calculated and divided by the sweep rate. The obtained value corresponds to the amount of charge that is transferred into creating an oxide, Q (often measured in C). Knowing the theoretical surface charge density for creating a certain oxide layer, k (the theoretical surface charge density for creating gold oxide is $482 \mu C/cm^2$ [29]), the surface area, A_{real}, can be calculated according

to Equation 5.

$$A_{real} = \frac{Q}{k} \tag{5}$$

The geometric surface area, $A_{geometric}$, for a circular electrode with a certain radius, r, is given by Equation 6.

$$A_{geometric} = \pi r^2 \tag{6}$$

The roughness factor, ρ, is the real surface area per unit geometric surface area. It is thus given by Equation 7. This factor expresses the relationship between the real surface area and the geometric surface area and thus it gives an idea of the degree of porosity. The higher the roughness factor, the more porous the surface area. Note that surface roughness and surface heterogeneity are two different concepts; the difference is that the former requires periodicity while the latter does not [30].

$$\rho = \frac{A_{real}}{A_{geometric}} \tag{7}$$

The real surface area of the electrode can be found where the end potential has its first maximum, i.e. before the steep increase in surface charge, see Figure 5.

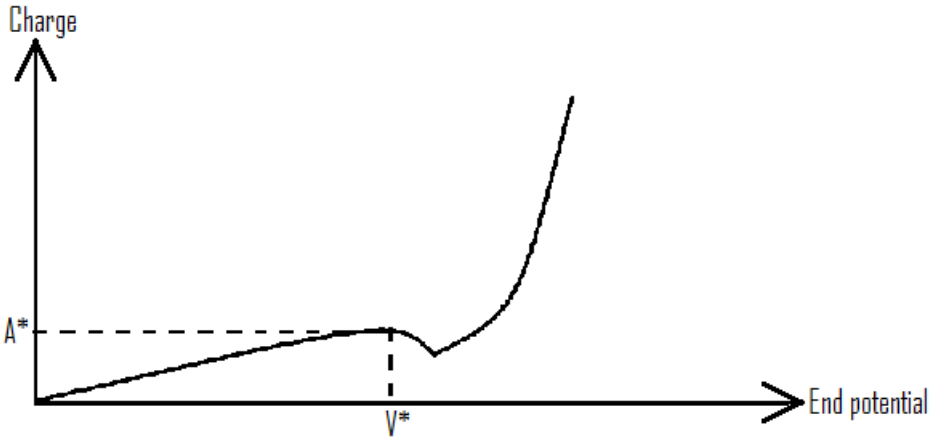

Figure 5: *Schematic drawing of the charge on the electrode surface as a function of the end potential. At V*, the largest achievable surface area, A*, can be found.*

The current I is defined as the variation of the charge Q over the time t. This can be written as Equation 8.

$$I = \frac{\mathrm{d}Q}{\mathrm{d}t} \tag{8}$$

This causes the charge to be expressed as Equation 9.

$$Q = \int_{t_i}^{t_f} I\mathrm{d}t \tag{9}$$

In the equation above, the adsorption starts at the time t_i and the monolayer is completed at the time t_f. When a potential V is applied to an electrode in the negative sweep during CV, this potential is given by the product of the potential sweep rate v by the time t subtracted from the initial potential V_0, see Equation 10.

$$V = V_0 - vt = V_0 - \frac{\mathrm{d}V}{\mathrm{d}t}t \tag{10}$$

The times forming the integral boudaries in Equation 9 are given by Equations 11 and 12.

$$t_i = \frac{V_0 - V_i}{v} \tag{11}$$

$$t_f = \frac{V_0 - V_f}{v} \tag{12}$$

Now, the charge can be written as Equation 13.

$$Q = \frac{1}{v}\int_{\frac{V_0-V_f}{v}}^{\frac{V_0-V_i}{v}} I\mathrm{d}V \tag{13}$$

By integrating the AUC for the reduction peak in the voltammetric curves, the real surface area (and therefrom the roughness factor) can be calculated [28].

6 Materials and methods

6.1 Chip design and fabrication

The gold electrodes to be fabricated had a diameter of $100\mu m$ and were connected to a square contact area with a side length of $1mm$ by a $4.5mm$ long, thin gold conductor, see Figure 6. One chip contained six of these units. These electrodes were larger than real neural electrodes (see Section 4.1.1) in order to simplify the handling of them and make them less sensitive.

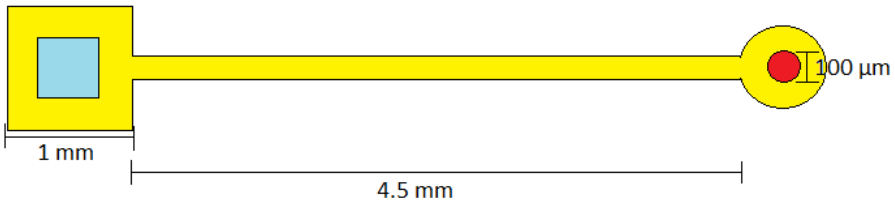

Figure 6: *Schematic drawing of the electrode connected to the contact area. The red circle in the figure is where the isolation has been opened up and thus it is the electrode. The blue square in the figure is the contact pad, where the isolation also has been opened up. The aluminum wire was attached to this contact pad. Note that the proportions are not made to scale.*

6.1.1 Description of the chip fabrication process

Silicon wafers were inserted into an oven (Thermco MB71) at $400°C$. The temperature was increased to $1050°C$ and the wafers were wet oxidized for about $6h$. In order to remove dirt from the surface of the wafers and to make it more reactive, the wafers were exposed to oxygen plasma (Diener FEMTO) for $5min$. After this cleaning, the wafers were inserted into an evaporator (Edwards Auto 306). A layer of $45nm$ titanium was evaporated and then a layer of $750nm$ gold was deposited on top of the titanium using electron beam evaporation. Because of the thick gold layer, all of the gold was not deposited in one run, since this could introduce pits and air cavities in the gold layer, creating stresses. Instead, five runs of $150nm$ gold layers each were deposited, waiting $10min$ between each run. In this way, the hot gold had time to fill in the pits.

The gold was structured using *UV* lithography. The positive resist AZ1514H (Microchemicals) was spun (Sitek) onto the wafers at a rate of $4000rpm$ for $1min$ and then they were soft baked on a $100°C$ hot plate (Sitek) for $1min$. The wafers were then exposed to *UV* light for $9s$ (Karl Suss MA4) and developed using 351 Developer (Microchemicals), diluted with *MilliQ* water (1 : 4), for $1min$ in order to remove the resist. Then the wafers were rinsed in two beakers

of *MilliQ* water. After this process, the patterns of the desired gold structure were left on the gold in the resist. The exposed gold was then etched using a gold etchant ($4g$ *KI* (Merck), $1g$ I_2 (Sigma-Aldrich), $40ml$ *MilliQ* water, etching rate of $100nm/20s$). The exposed titanium was etched using hydrofluoric acid (*HF*:*MilliQ* water at$1:5$) followed by a bath in *MilliQ* water. The wafers were then rinsed using acetone, ethanol and *MilliQ* water in order to remove the resist. After each water rinsing, the wafers were blown dry with nitrogen gas.

In order to isolate the gold conductor that connects the electrode to the contact pad and to pattern the final exposed area of the gold electrode and contact pad, a negative resist was used. First, the wafers were cleaned using oxygen plasma (Diener FEMTO) for $5min$ and after that, the negative resist SU8 2005 (Microchem) was spun (Sitek) onto the wafers at a rate of $4000rpm$ for $1min$, which gave a resist layer of about $5\mu m$. Then the wafers where soft baked in an oven (FN 300) at $86°C$ for $30min$ and let to cool down for $15min$. After soft baking, the wafers were exposed to *UV* light (Karl Suss MA4) for $13s$ and post-baked in an oven (FN 300) at $86°C$ for another $30min$. The wafers were let to cool down for $30min$ and developed in MR DEV600 (Microchem) for $1min$. Then they were rinsed in isopropanol and water and blown dry with nitrogen gas. Figure 7 shows the different fabrication steps. An optical microscope (Olympus BX40) was used to investigate the quality of the wafers.

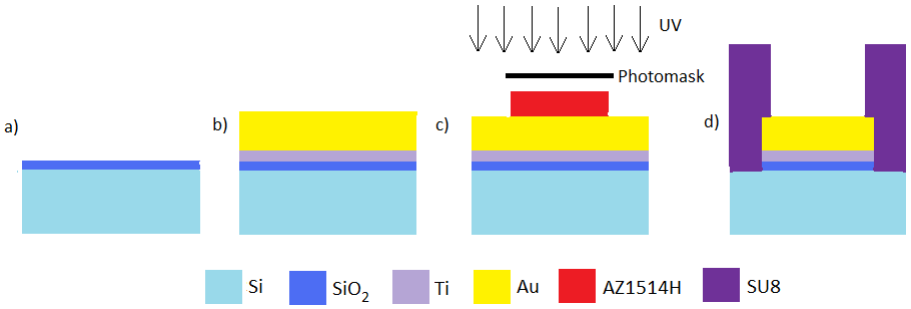

Figure 7: *Schematic drawing of the process steps in fabrication of the chips. a) Silicon dioxide is deposited onto a silicon substrate. b) Titanium and gold are evaporated onto the silicon dioxide layer. c) The substrate is covered by AZ1514H and UV radiated. d) SU8 provides the isolation and the gold electrode is exposed.*

Only one wafer was used for dicing chips. The wafer was diced (Micro Automation Model 602M) into chips containing six electrodes each. Then the chips were glued onto circuit boards and an aluminum wire with a diameter of $33\mu m$ was used to connect the gold and the copper, using a wirebond machine (Bausch & Lomb S−823), see Figure 8. To protect and isolate the wires, part of the samples were glued with a silicone (Elastosil A07).

Figure 9 shows a schematic drawing of the chip with electrodes on it, glued to

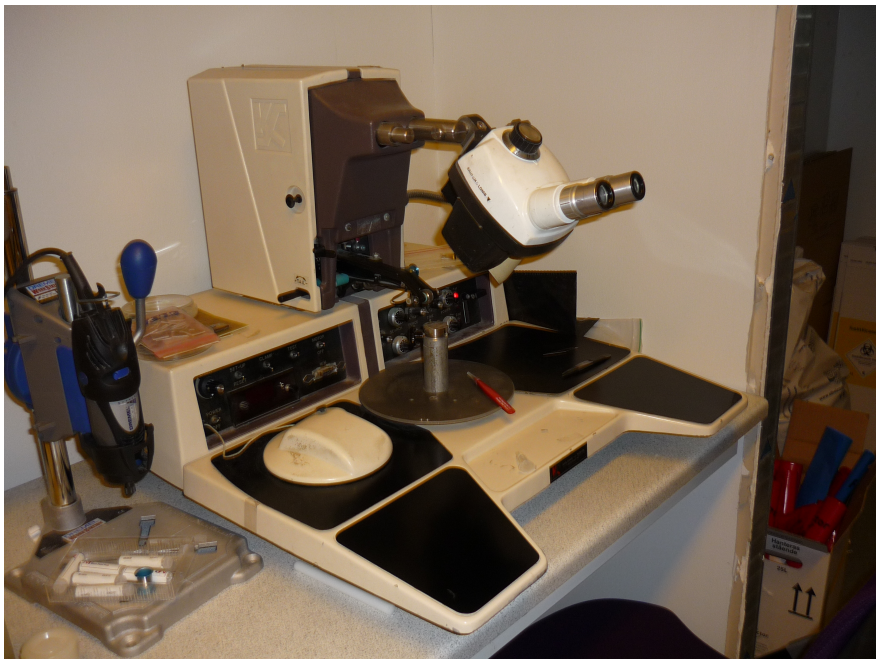

Figure 8: *Image of the wirebond machine.*

the circuit board and wirebonded, and Figure 10 shows four samples in different states.

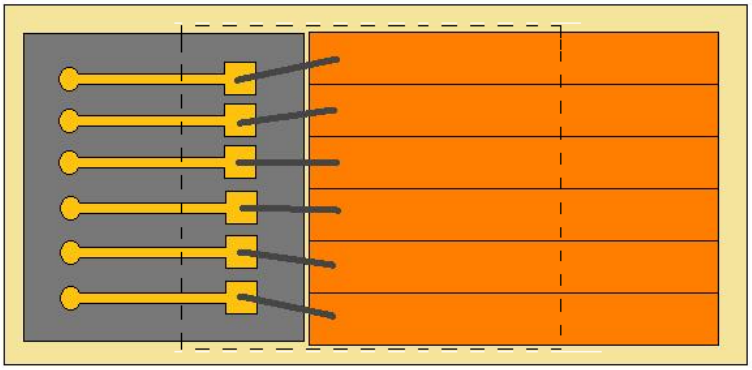

Figure 9: *Schematic drawing of the chip with electrodes connested to the circuit board. The bright yellow is gold, the lighter gray is silicon, the darker gray is aluminum, the honey coloured is copper and the pale yellow is plastic. The dashed lines mark out the area onto which the silicone was deposited. Note that the proportions are not made to scale.*

Figure 10: *Four samples in different states. From the left: a sputtered and copper taped sample with silicone, a copper taped sample with silicone, a sample with silicone (the blue plastic is protecting the electrodes from contamination) and an untreated sample.*

6.2 Anodization of the chips

To obtain a porous gold surface on the electrodes, both potentiostatic and galvanostatic anodizations were performed. During anodization, the gold electrode functioned as the anode and a platinum helical wire functioned as the cathode, see Figure 11. A reference electrode (silver/silver chloride) was used to control the applied potential. The electrolyte consisted of $0.5M$ oxalic acid (oxalic acid dihydrate, 99% purity, Sigma-Aldrich, *MilliQ* water) with a pH value between 0 and 1, measured with a lackmus paper. Figure 12 shows the setup for the anodization.

The apperature used for anodization included a potentiostat (Ivium CompactStat), working as a power supply and an amperemeter, with its own multiplexer system (Ivium MultiWE 32) and it was controlled from the manufacturer´s software (IviumSoft). All anodization experiments were performed at room temperature. After anodization, the electrodes where investigated with an optical microscope (Olympus BX40). This microscope was equipped with a camera

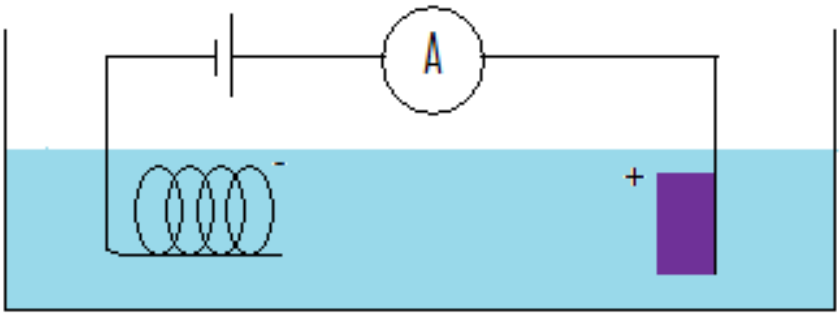

Figure 11: *Schematic drawing of a two-electrode experimental setup. The electrode to be anodized is the anode and the platinum wire is the cathode. However, in this experiment, a reference electrode was used too. Note that the proportions are not made to scale.*

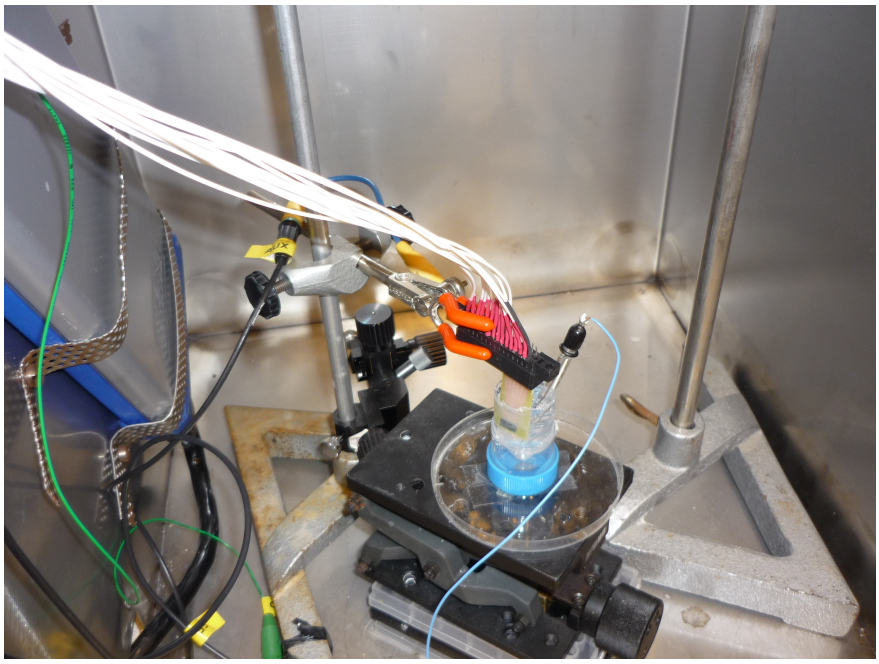

Figure 12: *Image of the setup for the anodization.*

(Edmund EO−5012C), which was used to take images of the electrodes at a magnification of $x20$.

6.2.1 Potentiostatic anodization

According to the patent published by Nishio and Masuda in 2010 [25] (see section 5.3.1), the potential applied to a gold electrode can be in the interval of $1.5 - 11V$. To start with, a lower potential of $1V$ was chosen, as a too high potential might damage the electrodes.

The anodization times were ranging from a few seconds up to several hours. On each chip, the first five electrodes were anodized for increasing time periods while the sixth electrode was kept as a reference. The anodization times tested were $5s$, $30s$, $2min$, $10min$, $30min$, $1h$, $2h$, $4h$, $6h$ and $9h$.

6.2.2 Galvanostatic anodization

In the aforementioned patent [25], it is also stated that the current density should be about $20 - 25mA/cm^2$. Here, it corresponds to a current of $1.5 - 1.875\mu A$. The lowest current in this range was chosen as a start value. The times were the same as for the potentiostatic anodization.

6.3 *SEM* preparation and imaging

Before the samples could be inserted into the *SEM*, they had to go through some pretreatment. First, most of the circuit board was covered with copper tape in order to avoid charging effects in the *SEM*. Then they were sputtered (Polaron E5100 DC) with approximately $10nm$ platinum in order to make the gold electrodes visible in the *SEM*. After this pretreatment, the electrodes were investigated in the *SEM* (Hitachi SU8010) and images were taken of each electrode. The voltage was $3.0kV$ and secondary electrodes were used.

6.4 Measurements at the best anodization values

According to the *SEM* images, the best combination of anodization mode and time seemed to be galvanostatic anodization at $1.5\mu A$ for $1h$ (see section 7.1). This constituted the start point for further attempts.

- Impedance measurement
- *CV*
- Galvanostatic anodization at $1\mu A$

- Impedance measurement
- *CV*

The anodization was performed on four of the six electrodes on the chip, for $45min$, $60min$, $75min$ and $90min$, respectively, while the other two electrodes were kept as references. The impedance measurements and *CVs*, on the other hand, were performed on all the electrodes. The second impedance measurement and *CV* was carried out in order to compare if the impedance and real surface area change after the anodization, and if the *CV* changes the impedance. Just like the anodization, both the impedance measurements and the *CVs* were performed using the Ivium system.

6.4.1 Impedance measurements

The impedance measurements were performed in $0.01M$ *PBS* (*phosphate buffered saline*, sodium perborate, Sigma-Aldrich, *MilliQ* water) with a pH value of approximately 7 (measured with a lackmus paper). The impedance was measured for all the electrodes on the chip. Since the impedance curves seemed a bit unstable (they looked different after anodization compared to those before anodization), one chip was used to only perform impedance measurements with different settings, both galvanostatic and potentiostatic. The most stable impedance measurement mode seemed to be the potentiostatic one, so this mode was used from now on.

6.4.2 Cyclic voltammetry

The *CV* was performed in $0.5M$ sulfuric acid (GPR Rectapur, 95% purity, *MilliQ* water) with a pH value between 0 and 1 (measured with a lackmus paper). For the *CV*, a four-electrode setup was performed. The start potential was set to $-0.2V$ and it was swept to various end potentials, namely $1.3V$, $1.4V$ and so on up to $2.2V$. Each potential step was $50mV$, the scan rate was $100mV/s$ and the number of cycles was 3.

According to Equation 5, the real surface area was calculated from the *AUC* of the reduction peak. The diameter of the circular electrode was $100\mu m$ (i.e. the radius was $50\mu m$), meaning their geometric surface area was approximately $7850\mu m^2$, or $7.85{\cdot}10^{-5}cm^2$ (see Equation 6). The roughness factor was calculated according to Equation 7.

6.5 Final test series

After some evaluation of different combinations of impedance measurements, anodization modes and CV measurements, a final test series was planned.

1. Impedance measurement
2. Anodization
3. Impedance measurement
4. CV

The most stable mode of impedance measurements seemed to be potentiostatic impedance measurement, see Section 6.4.1. As mentioned in Section 6.4, the best anodization mode-time combination seemed to be galvanostatic anodization at $1.5\mu A$ for $1h$. Though, a choice was made to anodize the electrodes at a lower current of $1\mu A$ for a little longer times. When CV was carried out at too high potentials, the gold seemed to extricate, so in the final test, the final end potential was lowered.

For the final test, a potentiostatic impedance measurement was carried out on each electrode. Then, the electrodes were anodized galvanostatically at a current of $1\mu A$ for different times, see Table 1. All six electrodes on each chip was anodized for the same times. After anodization, another potentiostatic impedance measurement was carried out and finally, CV measurements were carried out, going from $-0.2V$ up to $1.3V$, $1.4V$, $1.5V$ and $1.6V$, respectively. So finally, there were 12 electrodes per anodization time.

Number of electrodes	**Anodization time (min)**
12	60
12	75
12	90

Table 1: *The different anodization times in the final test and the number of electrodes anodized for each time.*

Since there were concerns that the theoretical surface charge density of $482\mu C/cm^2$ for creating gold oxide (see Section 5.5.1) was perhaps not valid in this case, CV was performed on a blank chip (all six electrodes) according to the same settings as for the other six chips. Out of the six electrodes on this chip, only two exhibited good CV graphs. The mean surface charge was calculated and divided by the geometric surface area of the electrode.

To calculate the real surface area of the electrodes, the calculation and simulation program MATLAB® R2104a (The MathWorks Inc., Natick, MA, 2014) was used to plot the current as a function of the potential. The real surface area could then be calculated by following the steps below:

1. Identify the reduction peak.
2. Mark out one coordinate on each side of this peak.
3. Take the y values in the coordinates (corresponding to the currents) and insert them into an integration function that gives the AUC $[A{\cdot}V]$.
4. Divide the AUC by the scan rate $[V/s]$ and obtain the surface charge $[A{\cdot}s = C]$.
5. Divide the surface charge by the surface charge density for creating gold oxide and this will give the real surface area.

To obtain the roughness factor, the real surface area was simply divided by the geometric surface area, according to Equation 7.

7 Results

7.1 The best combination of anodization mode and time

The anodization mode-time combination giving the best resulting surface structure was galvanostatic anodization at $1.5\mu A$ for $1h$, see Figure 13a. This can be compared to the surface structure of an electrode anodized in the same way, but for $2h$, see Figure 13b. The longer anodization time provided a similar porous surface as for the shorter time, but there were some fields where the gold had been removed, as can be seen in said figure. This gives a less effective electrode and there might be lack of contact between the "islands of gold". In other words, $2h$ was too long to anodize the electrode but $1h$ seemed like a reasonable anodization time for galvanostatic anodization at $1.5\mu A$.

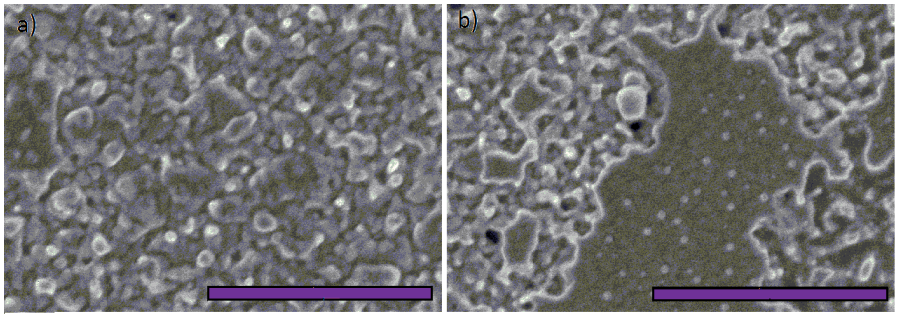

Figure 13: *The surface of an electrode anodized galvanostatically at* $1.5\mu A$ *for a)* $1h$ *and b)* $2h$*, respectively (scalebar* $= 1\mu m$*).*

7.2 Final test series

The results of the final test series are presented in Section 7.2.1−7.2.5. By the 12 electrodes tested for each anodization time, only some of them were good enough to be evaluated. For $60min$, only four of the electrodes were good enough, while nine electrodes anodized for $75min$ and seven electrodes anodized for $90min$ demonstrated adequate quality for evaluation.

7.2.1 Impedance measurements

Figure 14 shows the impedance as a function of frequency for the electrodes of adequate quality anodized for $60min$, $75min$ and $90min$, respectively. The mean impedance at each frequency (solid lines) is plotted together with the standard

deviation (dashed lines), both before (red curves) and after anodization (blue curves). The mean impedance and standard deviation before anodization are plotted for all 20 electrodes while the corresponding values after anodization are plotted for the corresponding anodization times. As can be seen in this figure, the impedance decreases sharply after anodization, meaning that the surface area has increased. Another aspect of the result is that the standard deviation is lowest for $60min$ and highest for $75min$.

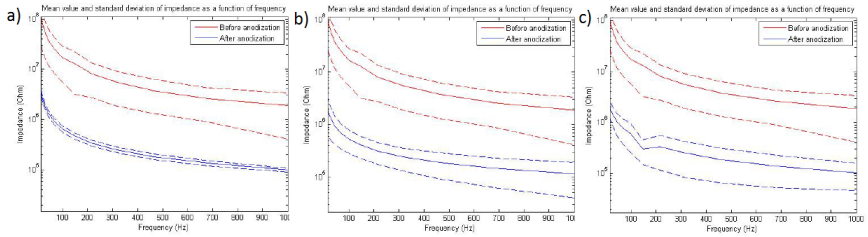

Figure 14: *Impedance as a function of frequency for the electrodes of adequate quality anodized for a)* $60min$ *(*$n = 4$*) b)* $75min$ *(*$n = 9$*) and c)* $90min$ *(*$n = 7$*), respectively. The red curve shows the impedance before anodization and the blue curve shows the impedance after anodization. The mean impedance for each frequency (solid lines) is plotted together with the standard deviation (dashed lines).*

7.2.2 Cyclic voltammetry

Figure 15 shows the CV graphs of an electrode anodized for $60min$, $75min$ and $90min$, respectively. As can be seen in this figure, two coordinates are marked out on the curve, one on each side of the reduction peak. The y values correspond to the currents, and they were inserted into an integration function giving the AUC. Since the current had the unit of nC and the potential had the unit of V, the unit of the AUC was $nC{\cdot}V$. In order to convert the AUC to the unit of nC (i.e. surface charge), the AUC was divided by 0.1, since the scan rate was $100mV/s = 0.1V/s$ ($C = A{\cdot}s$).

The mean surface charge calculated from the blank chip was $10.81nC$. Divided by the geometric surface area (which was approximately $7850\mu m^2$, see Section 6.4.2), it gave a surface charge density of approximately $138\mu C/cm^2$. This experimental surface charge density was used instead of the theoretical surface charge density of $482\mu C/cm^2$ when calculating the real surface area and roughness factor.

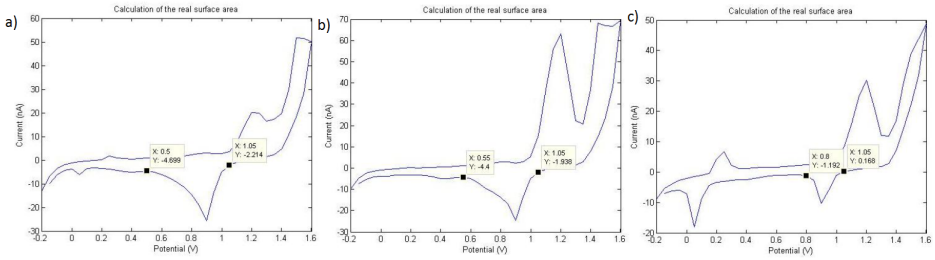

Figure 15: *The CV graph of an electrode anodized for a)* $60min$*, b)* $75min$ *and c)* $90min$*, respectively.*

7.2.3 The real surface area of the electrodes

Table 2 shows the approximate mean values and standard deviations for the real surface areas and roughness factors calculated for the electrodes anodized at $60min$, $75min$ and $90min$, respectively. As can be seen, these are largest for $75min$ and smallest for $60min$.

Anodization time	Mean surface area	Mean roughness factor
$60min$ $(n = 4)$	22500±12200 (μm^2)	2.87±1.55
$75min$ $(n = 9)$	59500±36800) (μm^2)	7.58±4.69
$90min$ $(n = 7)$	51500±30200 (μm^2)	6.56±3.85

Table 2: *The mean surface area and roughness factor and their standard deviations for the different anodization times in the final test.*

7.2.4 Surface structure

Figure 16 shows the surface structures at $x80k$ magnification for electrodes anodized for $60min$, $75min$ and $90min$, respectively.

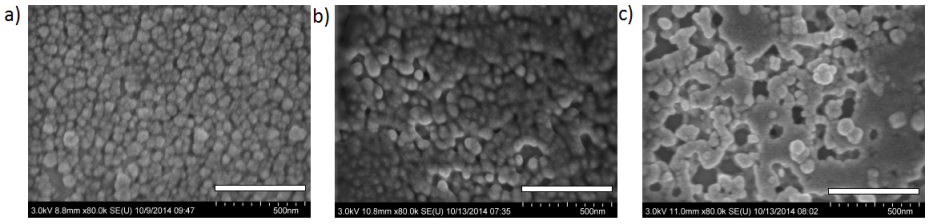

Figure 16: *SEM image of an electrode anodized for a)* $60min$*, b)* $75min$ *and c)* $90min$*, respectively (scalebar* $= 500nm$*).*

7.2.5 Colour changes

Among the electrodes of adequate quality, three of them had some colour change revealed by the optical microscope, see Figure 17a. This can be compared to Figure 17b, which shows no visible colour change (10 electrodes exhibited this appearance). Figure 17c shows an electrode with a heterogeneous colour change, which was experienced on the remaining seven electrodes. The magnification is $x20$.

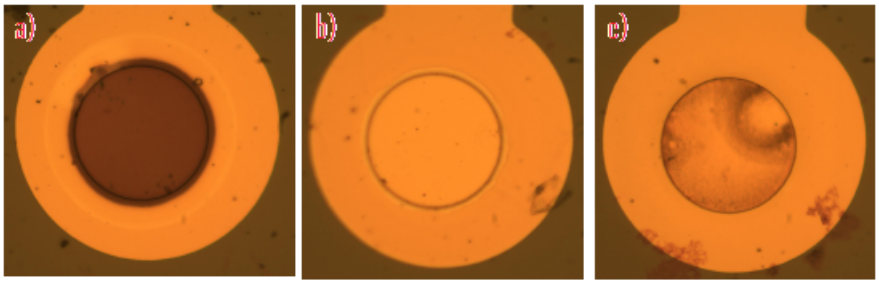

Figure 17: *Optical microscope images for three electrodes with different colour changes. The inner circle is the electrode (with a diameter of* $100\mu m$*). a) An electrode anodized for* $90min$*. The electrode had a colour change to dark red-brown. b) An electrode anodized for* $60min$*. The electrode did not visibly change colours. c) An electrode anodized for* $75min$*. The electrode gained a heterogeneous colour scale.*

8 Discussion

8.1 General

Since the aim of this project was to obtain gold electrodes with enlarged surface areas, the results are quite satisfying. In the final test series, the real surface area was increased for all three anodization times. However, out of the 36 electrodes anodized in this test series (12 electrodes per anodization time), only 20 of them where of adequate quality to be evaluated. From now on, only these 20 electrodes will be considered in the discussion.

The *SEM* images of the electrodes were in most cases not exhibiting any structure resembling the one in Figure 13a. Figure 16 shows some exceptions. Images taken with the optical microscope revealed a dark red-brown colour, almost black, for a few of the electrodes, see Figure 17a. This could indicate either a nanoporous gold surface (see Section 5.2) or that the gold had loosened from the electrode. In total, three of the electrodes (all of them anodized for $90min$) recieved this dark colour. Half of the electrodes showed no visible colour change, see Figure 17b. These where the four electrodes anodized for $60min$ and the remaining six electrodes were anodized for $75min$. The remaining seven electrodes (three of them anodized for $75min$ and the other four anodized for $90min$) also had colour changes, but of a more heterogeneous kind, see Figure 17c. The thickness of the gold layer is probably involved in the optimal anodization time, since it will take longer time to reduce a thick gold layer than a thin one.

The number of electrodes is on the low side, especially for $60min$, and in order to obtain safe results, more replicas would be needed.

8.2 Impedance measurements

For all three anodization times, the measured impedance was significantly lower after anodization than before anodization, which was a desired result since it indicates a larger surface area. The mean impedance for each frequency was plotted together with the standard deviation. As can be seen in Figure 14, the standard deviation after anodization is lowest for the electrodes anodized for $60min$ and highest for the electrodes anodized for $75min$, while it is intermediate for the electrodes anodized for $90min$. This seems proportional to the number of replicas.

8.3 Cyclic voltammetry

The *CV* graphs for the 20 good electrodes had a quite varying appearance. Some of them had very large oxidation and reduction peaks while some peaks were very small. In a few graphs, two reduction peaks could be seen (in these cases, the first reduction peak after the "turning back" from the end potential was used, see Figure 15c). Since the coordintes on each side of the reduction peak were chosen manually, perhaps the most optimal coordinates were not always chosen. This affects the AUC and thus, even the mean values and standard deviations of the real surface area and roughness factor.

The surface charge density determined experimentally was less than 30% of the theoretical surface charge density for creating gold oxide. This great difference may be due to some parameters that are not taken into account when calculating a theoretical surface charge density, since theoretical values assume ideal conditions, which is seldom the reality. Therefore, the experimental surface charge density should be used instead of the theoretical surface charge density. Also, when using the lower experimental surface charge density, the calculated real surface areas of the electrodes became larger than with the theoretical surface charge density.

The method for calculation of the real surface area described in Section 5.5.1, see Figure 5, was not used in this case. This was because it was not possible to go to such high maximum potential, since it would extricate the gold from the electrodes. That is why the real surface area was calculated in the way described in Sections 6.5 and 7.2.2−7.2.3.

8.4 The real surface area of the electrodes

The mean surface area and standard deviation is lowest for the electrodes anodized for $60min$ and highest for the electrodes anodized for $75min$ (and consequently, the same applies for the roughness factor). The electrodes anodized for $90min$ show an intermediate value in both mean surface area and standard deviation (hence the same for the roughness factor). This might be due to the anodization time being to high in the latter case, extricating the gold.

9 Conclusions and future work

Attempts to anodize circular gold electrodes with a diameter of $100\mu m$ in $0.5M$ oxalic acid in order to enlarge their surface areas have been made. Evaluation of the results using optical microscope, *SEM*, impedance measurement and *CV* shows that it seems possible to enlarge the surface area of gold electrodes using anodization in oxalic acid. The anodization mode was galvanostatic anodization at $1\mu A$ and the electrodes were anodized for $60min$, $75min$ and $90min$, respectively. Potentiostatic impedance measurements were performed and the *CV* was run from $-0.2V$ up to $1.3V$, $1.4V$, $1.5V$ and $1.6V$, respectively. The surface area was enlarged up to seven times.

However, the desire is to test this surface area enlargement technique on real neural electrodes, which have a geometric surface area of only about 0.15% of the geometric surface area of the test electrodes. The much smaller size makes the real neural electrodes more sensitive and more difficult to handle. To delimit the exposure to contamination, the whole procedure might have to be performed inside a cleanroom with a low *ISO* number, since the test electrodes (which were fabricated in a non-certified cleanroom and anodized in an ordinary laboratory) were exposed to contamination of a degree that would make real neural electrodes non-functional. But on the other hand, the test electrodes were just used to test a surface area enlargement technique, as the name suggests. Furthermore, since there is a large number of electrodes on a wafer, there will still be some usable electrodes even if some parts of the wafer is contamined. If the technique is viable for the test electrodes, it ought to be manageable to apply to real neural electrodes too.

In the future, this surface area enlargement technique will hopefully be tested on real neural electrodes, and if the results are good, the neural electrodes of the future will have potential to become more efficient than they are today. However, in order to have safe results, this technique should be tested on a larger number of test electrodes before it is performed on real neural electrodes and implanted into the brain of an animal or a human.

References

[1] D. Purves, G. J. Augustine, D. Fitzpatrick, W. C. Hall, A-S. LaMantia, J. O. McNamara and S. M. Williams, "Neuroscience", *Sinauer Associates, Inc. Third Edition*, pp 31 – 35, 2004

[2] A. P. Alivisatos, A. M. Andrews, E. S. Boyden, M. Chun, G. M. Church, K. Deisseroth, J. P. Donoghue, S. E. Fraser, J. Lippincott-Schwartz, L. L. Looger, S. Masmanidis, P. L. McEuen, A. V. Nurmikko, H. Park, D. S. Peterka, C. Reid, M. L. Roukes, A. Scherer, M. Schnitzer, T. J. Sejnowski, K. L. Shepard, D. Tsao, G. Turrigiano, P. S. Weiss, C. Xu, R. Yuste and X. Zhuang, "Nanotools for Neuroscience and Brain Activity Mapping", *ACS Nano*, vol. 7, no. 3, pp 1850 – 1866, Mar. 2013

[3] Neuronano Research Center, *www.med.lu.se/nrc*, Retrieved: 2014 – 06 – 17

[4] G. James, R. C. James, A. A. Alchian, E. F. Beckenbach, C. Bell, H. V. Craig, A. D. Michal and I. S. Sokolnikoff, "Mathematics Dictionary", *van Nostrand Reinhoold Company, Fourth Edition*, pp 180, 1976

[5] J. Nissa, "Fabrication of a porous anodic alumina membrane", *Master´s Thesis at Lund University, Faculty of Engineering*, pp 3, May 2013

[6] B. Ilic, D. Czaplewski, P. Neuzil, T. Stanczyk, J. Blough and G. J. Maclay, "Preparation and characterization of platinum black electrodes", *Journal of Materials Science*, vol. 35, no. 14, pp 3447 – 3457, 2000

[7] Y. Yang, Y. Xia, W. Huang, J. Zheng and Z. Li, "Fabrication of nano-network gold films via anodization of gold electrode and their application in SERS", *Journal of Solid State Electrochemistry*, vol. 16, pp 1733 – 1739, Nov. 2011

[8] G. Zhong, A. Liu, X. Chen, K. Wang, Z. Lian, Q. Liu, Y. Chen, M. Du and X. Lin, "Electronchemical biosensor based on nanoporous gold electrode for detection of PML/RARα fusion gene", *Biosensors and Bioelectronics*, vol. 26, pp 3812 – 3817, Mar. 2011

[9] J. Biener, A. Wittstock, L. A. Zepeda-Ruiz, M. M. Biener, V. Zielasek, D. Kramer, R. N. Viswanath, J. Weissmüller, M. Bäumer and A. V. Hamza, "Surface-chemistry-driven actuation in nanoporous gold", *Nature Materials*, vol. 8, no. January 2009, pp 47 – 51, Nov. 2008

[10] J. Patel, L. Radhakrishnan, B. Zhao, B. Uppalapati, R. C. Daniels, K. R. Ward and M. M. Collinson, "Electrochemical Properties of Nanostructured Porous Gold Electrodes in Biofouling Solutions", *Analytical Chemistry*, no. 85, pp 11610 – 11618, Nov. 2013

[11] M. M. Collinson, "Nanoporous Gold Electrodes and Their Applications in Analyical Chemistry", *ISRN Analytical Chemistry*, vol. 2013, pp 1 – 21, Dec. 2012

[12] F. Jia, C. Yu, Z. Ai and L. Zhang, "Fabrication of Nanoporous Gold Film Electrodes with Ultrahigh Surface Area and Electrochemical Activity", *Chemistry of Materials*, vol. 19, no. 15, pp 3648 – 3653, May 2007

[13] X. Quan, L. M. Fischer, A. Boisen and M. Tenje, "Development of nanoporous gold electrodes for electrochemical applications", *Microelectronic Engineering*, vol. 88, pp 2379 – 2382, Jan. 2011

[14] E. Seker, Y. Berdichevsky, M. R. Begley, M. L. Reed, K. J. Staley and M. L. Yarmush, "The fabrication of low-impedance nanoporous gold multiple-electrode arrays for neural electrophysiology studies", *Nanotechnology*, vol. 21, no. 2010, pp 1 – 7, Mar. 2010

[15] R. Jurczakowski, C. Hitz and A. Lasia, "Impedance of porous Au based electrodes", *Journal of Electroanalytical Chemistry*, vol. 572, pp 355 – 366, Feb. 2004

[16] K. Koga, T. Ikeshoji and K. Sugawara, "Size- and Temperature-Dependent Structural Transistions in Gold Nanoparticles", *Physical Review Letters*, vol. 92, no. 11, pp 115507 – 1 – 4, Mar. 2004

[17] IUPAC, *Compendium of Chemical Terminology*, 2*nd* ed. (the "Gold Book"), 1997. Online corrected version: 2006– "faradaic current". Retrieved 2014 – 04 – 01

[18] R. Jurczakowski, C. Hitz and A. Lasia, "Impedance of porous gold electrodes in the presence of electroactive species", *Journal of Electroanalytical Chemistry*, vol. 582, pp 85 – 96, Apr. 2005

[19] P. B. Bélanger, E. L. Adler and N. C. Rumin, "Introduction to Circuits with Electronics: An Integrated Approach", *Holt-Saunders International Editions*, pp 5, 1985

[20] S. Xu, Y. Yao, P. Wang, Y. Yang, Y. Xia, J. Liu, Z. Li and W. Huang, "Anodic Fabrication of Nanoporous Gold Films from Pure Gold in Oxalic Acid Solution and Their Applications in Electrocatalysis and SERS", *International Journal of Electrochemical Science*, vol. 8, pp 1863 – 1870, Feb. 2013

[21] K. Nishio and H. Masuda, "Anodization of Gold in Oxalate Solution To Form a Nanoporous Black Film", *Angewandte Chemie (International ed. in English)*, vol. 123, pp 1641 – 1645, Jan. 2011

[22] A. Gutiérrez, J. Giraldo and M. E. Rodríguez-García, "Temporal Evolution of Anodization Current of Porous Silicon Samples", *Materials Sciences and Applications*, vol. 4, pp 43 – 47, Aug. 2013

[23] D. van Noort and C-F. Madenius, "Porous gold surfaces for biosensor application", *Biosensors and Bioelectronics*, vol. 15, no. 3 – 4, pp 203 – 209, Jun. 2000

[24] S. Shukla, A. Priscilla, M. Banerjee, R. R. Bhonde, J. Ghatak, P. V. Satyam and M. Sastry, "Porous Gold Nanospheres by Controlled Transmetalation Reaction: A Novel Material for Application in Cell Imaging", *Chemistry of Materials*, vol. 17, no. 20, pp 5000 – 5005, Sep. 2005

[25] K. Nishio and H. Masuda, "Porous gold materials and production methods", *United States Patent Application Publication*, no. *US*2010/0230287*A*1, pp 1 – 9, Sep. 2010

[26] S. K. Mondal, K. R. Prasad and N. Munichandraiah, "Analysis of electrochemical impedance of polyaniline films prepared by galvanostatic, potentiostatic and potentiodynamic methods", *Synthetic Metals*, vol. 148, pp 275 – 286, 2005

[27] P. T. Kissinger and W. R. Heineman, "Cyclic Voltammetry", *Journal of Chemical Education*, vol. 60, no. 9, pp 702 – 706, Sep. 1983

[28] J. M. Doña, J. A. Herrera Melián and J. Pérez Peña, "Determination of the Real Surface Area of Pt Electrodes by Hydrogen Adsorption Using Cyclic Voltammetry", *Journal of Chemical Education*, vol. 77, no. 9, pp 1195 – 1197, Sep. 2000

[29] J. C. Hoogvliet, M. Dijksma, B. Kamp and W. P. van Bennekom, "Electrochemical Pretreatment of Polycrystalline Gold Electrodes To Produce a Reproducible Surface Roughness for Self-Assembly: A Study in Phosphate Buffer pH 7.4", *Analytical Chemistry*, vol. 72, no. 9, pp 2016 – 2021, May 2000

[30] S. Trasatti and O. A. Petrii, "Real surface area measurements in electrochemistry", *Journal of Electroanalysis and Chemistry*, vol. 327, pp 353−376, 1992